Available online at www.sciencedirect.com
SCIENCE DIRECT
Journal of Organometallic Chemistry 691 (2006) 2448–2456
Journal of Organometallic Chemistry
www.elsevier.com/locate/jorganchem

Substitution derivatives of the heteronuclear cluster $RuOs_3(\mu\text{-}H)_2(CO)_{13}$: Monosubstituted group 15 derivatives

Leonard Joachim Pereira, Weng Kee Leong *

Department of Chemistry, National University of Singapore, Kent Ridge, Singapore 119260, Singapore

Received 29 November 2005; received in revised form 11 January 2006; accepted 12 January 2006
Available online 23 February 2006

Abstract

Tertiary group 15 ligand monosubstituted derivatives of the heteronuclear cluster $RuOs_3(\mu\text{-}H)_2(CO)_{13}$ have been prepared and their solid state and solution structures examined. A number of isomeric structural types have been identified in solution, and these appear to be correlated to disorder in the solid state. Hydride fluxionality and restricted rotation about the metal–phosphorus bond have also been observed.

Keywords: Heterometallic complexes; Ruthenium; Osmium; Phosphanes

1. Introduction

Heteronuclear clusters are of interest as the presence of different transition metal atoms in close proximity has the potential to effect novel reactions via synergistic interactions. One interesting family of heteronuclear clusters is tetranuclear clusters of the formulae $M'M_3(\mu\text{-}H)_2(CO)_{13}$, where M and M′ are the group 8 elements; three members of this family are known, viz., $FeRu_3(\mu\text{-}H)_2(CO)_{13}$, $FeOs_3(\mu\text{-}H)_2(CO)_{13}$ and $RuOs_3(\mu\text{-}H)_2(CO)_{13}$ (**1**); an unsuccessful attempts have also been made on the preparations of the remaining members of this series, viz., the clusters $MFe_3(\mu\text{-}H)_2(CO)_{13}$ (where M = Ru, Os) [1]. The chemistry of the first two members of this series has been fairly well investigated [2]; insofar as phosphine substitution chemistry is concerned, that of $FeRu_3(\mu\text{-}H)_2(CO)_{13}$ has been investigated in quite great detail by Geoffroy and coworkers [3]. The monosubstituted derivatives $FeRu_3(\mu\text{-}H)_2(CO)_{12}(PR_3)$ have the phosphorus ligand on a ruthenium vertex and in solution, there is rapid interconversion between two isomers that differ in the relative disposition of the phosphorus ligand with respect to the carbonyl and hydride ligands; a third, minor isomer which is believed to have the phosphine substituted at the iron was also reported [3a]. The photochemical substitution reaction of $FeOs_3(\mu\text{-}H)_2(CO)_{13}$ with PPh_3 has also been reported although the product has not been structurally characterized [4].

In contrast, the chemistry of **1** has been much less investigated. It is well known that in the iron triad, the chemistries of ruthenium and osmium are much more alike than they are to that of iron. Thus we have undertaken a series of investigations into the chemistry of $RuOs_3(\mu\text{-}H)_2(CO)_{13}$ and its derivatives, especially in comparison to those established for $FeRu_3(\mu\text{-}H)_2(CO)_{13}$. In this and an accompanying article, we would like to report our investigations into the solid-state and solution structures of the group 15 ligand-substituted derivatives $RuOs_3(\mu\text{-}H)_2(CO)_{12}(L)$ and $RuOs_3(\mu\text{-}H)_2(CO)_{11}(L)_2$ (where L = tertiary group 15 ligand).

2. Experimental

2.1. General procedures

All reactions and manipulations were carried out under nitrogen by using standard Schlenk techniques. Solvents were purified, dried, distilled, and stored under nitrogen prior to use. Routine NMR spectra, T_1 determinations and inverse-gated decoupled ^{31}P NMR spectra were acquired on a Bruker ACF300 NMR spectrometer. Selec-

* Corresponding author.
E-mail address: chmlwk@nus.edu.sg (W.K. Leong).

0022-328X/$ - see front matter © 2006 Elsevier B.V. All rights reserved.
doi:10.1016/j.jorganchem.2006.01.028

tive decoupling experiments and 2D NMR spectra were acquired on a Bruker Avance DRX500 or Bruker AMX500 machine. EXSY spectra were recorded with a mixing time of 0.5 s unless otherwise stated. The solvent used was deuterated chloroform unless otherwise stated. Chemical shifts reported are referenced to that for the residual proton of the solvent for ^{1}H, and to 85% aqueous H_3PO_4 (external standard) for ^{31}P. Mass spectra were obtained on a Finnigan MAT95XL-T spectrometer in an *m*-nitrobenzyl alcohol matrix. Microanalyses were carried out by the microanalytical laboratory at the National University of Singapore. The preparation of cluster **1** appears in our earlier report [5]. All other reagents were from commercial sources and used as supplied.

2.2. Preparation of $RuOs_3(\mu\text{-}H)_2(CO)_{12}(L)$ (**2**) and $RuOs_3(\mu\text{-}H)_2(CO)_{11}(L)_2$ (**3**)

The preparation of $RuOs_3(\mu\text{-}H)_2(CO)_{12}(EPh_3)$ (**2a**–**c**) and $RuOs_3(\mu\text{-}H)_2(CO)_{11}(EPh_3)_2$ (**3a**–**c**) (where E = P, As or Sb, respectively) have been previously described [5,6]. A similar procedure was employed in the preparation of the other mono- and disubstituted derivatives with the following ligands:

P(n-Bu)$_3$: $RuOs_3(\mu\text{-}H)_2(CO)_{12}(P^nBu_3)$ (**2d**). Yield = 38%; ν_{CO}/cm^{-1} (hexane) 2093m, 2062vs, 2039vs, 2022s, 2009m, 2001mw, 1994mw, 1990mw, 1978w, 1969w. MS: 1211.7 (M^+). Anal. Calc. for $C_{24}H_{29}O_{12}Os_3PRu \cdot C_6H_{14}$: C, 27.75; H, 3.34. Found: C, 27.5; H, 3.23%.

$RuOs_3(\mu\text{-}H)_2(CO)_{11}\{P(n\text{-}Bu)_3\}_2$ (**3d**). Yield = 10%; ν_{CO}/cm^{-1} (hexane) 2073s, 2061w, 2039vs, 2008s, 1986mw, 1980mw, 1965m, 1765mw, 1721mw. MS: 1387.

P(t-Bu)$_3$: $RuOs_3(\mu\text{-}H)_2(CO)_{12}(P^tBu_3)$ (**2e**). Yield = 55%; ν_{CO}/cm^{-1} (hexane) 2095mw, 2077vw, 2054vs, 2022ms, 2005mw, 1996mw, 1976vw, 1961w. MS: 1212 (M^+). Anal. Calc. for $C_{24}H_{29}O_{12}Os_3PRu \cdot \frac{1}{2}C_6H_{14}$: C, 25.83; H, 2.89. Found: C, 25.66; H, 3.05%.

PCy$_2$Ph: $RuOs_3(\mu\text{-}H)_2(CO)_{12}(PCy_2Ph)$ (**2f**). Yield = 45%; ν_{CO}/cm^{-1} (hexane) 2092m, 2062vs, 2038vs, 2022s, 2008m, 2000mw, 1988mw, 1976w, 1968w, 1726w, br. MS: 1284.1 (M^+). Anal. Calc. for $C_{30}H_{29}O_{12}Os_3PRu$: C, 28.06; H, 2.26. Found: C, 28.11; H, 2.22%.

$RuOs_3(\mu\text{-}H)_2(CO)_{11}(PCy_2Ph)_2$ (**3f**). Yield = 19%; ν_{CO}/cm^{-1} (hexane) 2074s, 2062w, 2040vs, 2007s, 1964m, 1728m, br. MS: 1531 (M^+). Anal. Calc. for $C_{47}H_{56}O_{11}Os_3P_2Ru$: C, 36.89; H, 3.67. Found: C, 37.05; H, 3.78%.

PCy$_3$: $RuOs_3(\mu\text{-}H)_2(CO)_{11}(PCy_3)$ (**2g**). Yield = 62%; ν_{CO}/cm^{-1} (hexane) 2091m, 2061vs, 2038vs, 2020s, 2007m, 1998mw, 1989mw. MS: 1289.8 (M^+). Anal. Calc. for $C_{30}H_{35}O_{12}Os_3PRu$: C, 27.93; H, 2.71. Found: C, 27.73; H, 2.81%.

PMe$_3$: $RuOs_3(\mu\text{-}H)_2(CO)_{12}(PMe_3)$ (**2h**). Yield = 55%; ν_{CO}/cm^{-1} (hexane) 2094m, 2063vs, 2055mw, 2039vs, 2023s, 2010m, 1994m, 1971w. MS: 1086.7 (M^+). Anal. Calc. for $C_{15}H_{11}O_{12}Os_3PRu$: C, 16.59; H, 1.02. Found: C, 16.69; H, 0.81%.

P(C$_6$F$_5$)$_3$: $RuOs_3(\mu\text{-}H)_2(CO)_{12}\{P(C_6F_5)_3\}$ (**2i**). Yield = 42%; ν_{CO}/cm^{-1} (hexane) 2100m, 2073vs, 2063vs, 2051vs, 2043s, 2018s, 2006s, 1994w, 1806w. MS: 1541.5 (M^+). Anal. Calc. for $C_{30}H_2F_{15}O_{12}Os_3PRu \cdot 1.5$toluene: C, 28.83; H, 0.84. Found: C, 28.80; H, 1.00%.

Presence of solvents in the samples were verified by ^{1}H NMR spectroscopy.

2.3. Crystal structure determinations

Crystals were mounted on quartz fibres. X-ray data were collected on a Bruker AXS APEX system, using Mo Kα radiation, with the SMART suite of programs [7]. Data were processed and corrected for Lorentz and polarisation effects with SAINT [8], and for absorption effects with SADABS [9]. Structural solution and refinement were carried out with the SHELXTL suite of programs [10]. Atomic coordinates are given in the Supporting Information; crystal and refinement data are listed in Table 1.

The structures were solved by direct or Patterson methods to locate the heavy atoms, followed by difference maps for the light, non-hydrogen atoms. Organic hydrogen atoms were placed in calculated positions and refined with a riding model. The metal hydrides were either located by low angle difference maps (**2e** and **2f**) or placed by potential energy calculations with the program XHYDEX [11]. The hydrides were given fixed isotropic thermal parameters and the M–H distance fixed at 1.84 Å. With the exception of those mentioned below involving disordered parts, all non-hydrogen atoms were given anisotropic thermal parameters in the final model. Refinements were on $\sum[w(F_o^2 - F_c^2)^2]$.

The clusters **2b** and **2f** exhibited disorder of the metal core. Each disordered site was modelled with a partial osmium and ruthenium, given identical anisotropic thermal parameters and positions, with sum of the occupancies of ruthenium over all sites restrained to 1.0. In **2b**, the disorder was modelled over all four metal sites. In **2f**, this was modelled over three metal sites; the Ru occupancies were fixed at 5%, 5% and 90% after refinement with an all-isotropic model. There was also disorder of phenyl over cyclohexyl rings for two sites in **2f**, which were modelled with fixed occupancies and the same isotropic thermal parameters for atoms at the same corresponding site. Appropriate restraints were applied; all the C atoms in **2f** were assigned isotropic thermal parameters. A disordered dichloromethane solvate molecule was found in **2e**, which was modelled accordingly with restraints as appropriate.

3. Results and discussion

We recently reported a high yield route to **1**, and the observation of three isomers in solution [5]. We had then been unable to assign a definite structure to the one isomer that showed two hydride resonances (Fig. 1). One problem was that the $^2J_{HH}$ was expected to be small [3], and hence the absence of any such coupling could not be taken to indicate that the correct structure was B′.

Recently, however, Aime et al. have shown that T_1 measurements may be useful for discriminating between such

Table 1
Crystal data for **2b–f** and **2i**

Compound	**2b**	**2c**	**2d**	**2e**	**2f**	**2i**
Empirical formula	$C_{30}H_{17}AsO_{12}Os_3Ru$	$C_{30}H_{17}O_{12}Os_3RuSb \cdot \frac{1}{2}CH_2Cl_2$	$C_{24}H_{29}O_{12}Os_3PRu$	$C_{24}H_{29}O_{12}Os_3PRu \cdot \frac{1}{2}CH_2Cl_2$	$C_{30}H_{29}O_{12}Os_3PRu$	$C_{30}H_2F_{15}O_{12}Os_3PRu$
Formula weight	1316.03	1447.78	1212.11	1254.57	1284.17	1541.96
Temperature (K)	293(2)	293(2)	293(2)	173(2)	223(2)	293(2)
Crystal system	Triclinic	Monoclinic	Triclinic	Monoclinic	Triclinic	Triclinic
Space group	$P\bar{1}$	$P2_1/n$	$P\bar{1}$	$P2_1/c$	$P\bar{1}$	$P\bar{1}$
a (Å)	10.1742(2)	8.9099(1)	9.0646(2)	15.0897(1)	9.9994(4)	11.8010(2)
b (Å)	12.8185(2)	28.1107(1)	11.7960(2)	9.1316(1)	11.3517(5)	12.7102(2)
c (Å)	13.4858(2)	14.8486(2)	17.0745(2)	24.4240(1)	16.4307(7)	13.5590(2)
α (°)	90.2640(10)	90	104.86	90	74.266(1)	95.740(1)
β (°)	91.5820(10)	95.4200(10)	94.7530(10)	90.922(1)	76.829(1)	95.304(1)
γ (°)	102.4460(10)	90	108.81	90	80.561(1)	112.593(1)
Volume (Å^3)	1716.70(5)	3702.42(7)	1642.84(5)	3365.02(5)	1737.52(13)	1849.21(5)
Z	2	4	2	4	2	2
ρ_c (g cm^{-3})	2.546	2.597	2.450	2.476	2.455	2.769
μ(Mo Kα) (mm^{-1})	12.513	11.579	12.117	11.913	11.465	10.854
F(000)	1196	2632	1112	2308	1184	1400
Crystal size (mm^3)	$0.30 \times 0.24 \times 0.08$	$0.18 \times 0.08 \times 0.06$	$0.38 \times 0.36 \times 0.14$	$0.36 \times 0.30 \times 0.06$	$0.19 \times 0.10 \times 0.04$	$0.360 \times 0.130 \times 0.08$
θ Range (°)	2.05 to 29.32	2.00 to 29.42	2.41 to 29.42	2.13 to 29.20	2.01 to 28.27	2.00 to 29.23
Reflections collected	13918	24181	35145	26030	21666	13992
Independent reflections [R_{int}]	8190 [0.0619]	9276 [0.0857]	7905 [0.0398]	8391 [0.0618]	8237 [0.0389]	8710 [0.0236]
Maximum and minimum transmission	0.200 and 0.019	0.560 and 0.248	0.297 and 0.099	0.493 and 0.236	0.657 and 0.219	0.461 and 0.234
Data/restraints/parameters	8190/5/434	9276/4/457	7905/4/376	8391/0/397	8237/45/284	8710/4/565
Goodness-of-fit on F^2	0.937	1.015	1.100	0.991	1.051	1.110
Final R indices [$I > 2\sigma(I)$]	$R_1 = 0.0749$, $wR_2 = 0.1787$	$R_1 = 0.0657$, $wR_2 = 0.1308$	$R_1 = 0.0510$, $wR_2 = 0.1339$	$R_1 = 0.0327$, $wR_2 = 0.0691$	$R_1 = 0.0389$, $wR_2 = 0.0841$	$R_1 = 0.0371$, $wR_2 = 0.0919$
R indices (all data)	$R_1 = 0.1134$, $wR_2 = 0.1968$	$R_1 = 0.1297$, $wR_2 = 0.1638$	$R_1 = 0.0621$, $wR_2 = 0.1403$	$R_1 = 0.0444$, $wR_2 = 0.0715$	$R_1 = 0.0478$, $wR_2 = 0.0881$	$R_1 = 0.0517$, $wR_2 = 0.1008$
Largest difference in peak and hole (e Å^{-3})	4.656 and −3.944	1.885 and −3.251	2.271 and −3.179	2.056 and −2.779	1.968 and −0.772	1.120 and −1.802

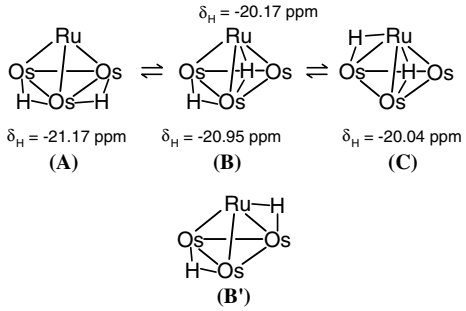

Fig. 1. Possible structures of the isomers of **1** and their tentative ^{1}H resonance assignments.

structures [12]. It may be expected that the larger inter-hydride distance in B′ should give rise to significantly longer T_1's for the hydrides in comparison to those in A or C, while B should have comparable T_1's. We have measured the T_1's to be 1.18(3) and 1.41(2) s for the resonances at δ_H −20.17 and −20.95 ppm, respectively. These values were not very different from the 1.48(4) and 1.26(9) s for that in A and C, respectively, suggesting that the structure B was indeed correct.

The reaction of **1** with various phosphorus ligands under TMNO activation generally afforded a mixture of the mono- and disubstituted derivatives; that for the ligands EPh_3 (E = P, As, Sb) have been reported earlier. The degree of success, however, varied with the identity of the ligand used. For most of the phosphines, both types of derivatives have been characterised but in the case of $^tBu_3P$ and $(C_6F_5)_3P$, only the monosubstituted derivatives were identified while the phosphites, $P(OR)_3$ (R = Me, Et, Ph), afforded air-sensitive red oils.

3.1. Solid-state structures

The single crystal X-ray structures of eight monosubstituted derivatives have been determined. Of these, the structures of the two isomeric forms of the PPh_3 monosubstituted derivative, viz., *Os*-$RuOs_3(\mu\text{-}H)_2(CO)_{12}(PPh_3)$, ***Os*–2a**, and *Ru*–$RuOs_3(\mu\text{-}H)_2(CO)_{12}(PPh_3)$, ***Ru*–2a**, have been reported previously [5]. The structures of the remaining compounds are reported here.

Of the eight monosubstituted derivatives, the structures of ***Os*–2a** and the $AsPh_3$ and PCy_2Ph derivatives, **2b** and **2f**, exhibited significant disorder of the heavy atoms. A detailed examination of the positions of the heavy atoms, group 15 atoms, and hydrides, show that six of the structures have essentially the same relative dispositions of these ligands. In their study on bridging, semibridging and terminal carbonyls, Crabtree and Lavin had found that the terminal, bent semibridging and symmetrically bridging carbonyls constituted a smooth continuum [13]. Our observations here are in agreement with that, and of the twelve CO ligands in each of our monosubstituted clusters, ten of them (nine in the case of **2i**) have ∠MCO close to linearity, up to ∼174°, and are clearly terminal CO ligands. The remaining two CO ligands (three in **2i**), with ∠MCO < 174°, are considered to be bridging and, except for **2e** and **2i**, they are to be found along the same metal–metal edges (Ru(4)–Os(2) and Ru(4)–Os(3)). The ORTEP plot showing the molecular structure of **2d**, which is representative of these six nearly isostructural compounds, is shown in Fig. 2. A common numbering scheme, together with selected bond parameters and the stereoelectronic parameters of the group 15 ligands, for these six structures are collected in Table 2.

What is immediately noticeable from the table is that the two longest metal–metal bonds are associated with bridging hydrides, and the longer of these is *cis* to the group 15 ligands. This appears to be true also for ***Os*–2a** in which the two hydrides span Os–Os bonds which at 2.9714(8) and 2.9371(7) Å are longer than the other metal–metal bonds, and the longer of the two is closer to the phosphorus atom (∠P(5)–Os(1)–Os(2) = 109.70(8)° and ∠P(5)–Os(1)–Os(3) = 115.86(9)°, respectively). The compound ***Os*–2a** is incidentally also the only monosubstituted derivative with the group 15 ligand at an osmium vertex that has been characterised crystallographically.

For **2e**, the two hydrides span Ru–Os bonds and they are also the two longest bonds (3.0045(5) and 2.9731(5) Å for Ru(4)–Os(2) and Ru(4)–Os(1), respectively) although here the phosphine seems to be closer to Os(1) than to Os(2) (∠P(5)–Ru(4)–Os(2) = 118.34(4)° and ∠P(5)–Ru(4)–Os(1) = 117.54(4)°, respectively) albeit only barely (Fig. 3). This lengthening is consistent with similar observations in the homometallic trinuclear systems; on the other hand, there does not appear to be any clear correlation between *d*(Ru–E) or ∠E–Ru–Os(1) with either the cone angle or electronic parameter [14].

An examination of the structural types adopted shows that group 15 ligand substitution is overwhelmingly at the Ru vertex. This preference for substitution at an Ru vertex cannot be merely statistical since that would have led to a 3:1 preference for substitution at an Os vertex.

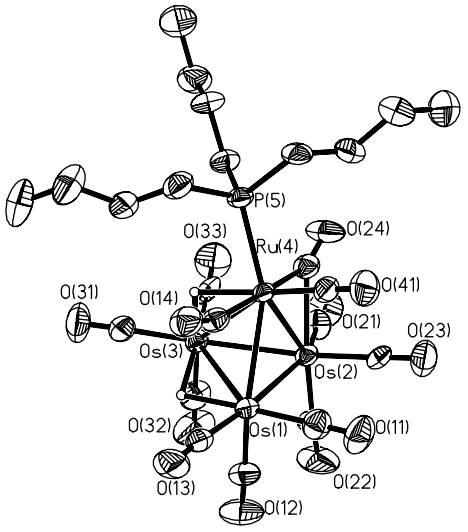

Fig. 2. ORTEP diagram of **2d** (50% thermal ellipsoids) with organic hydrogen atoms omitted.

Table 2
Common atomic numbering scheme and selected bond parameters for ***Ru*–2a**, **2b**, **2c**, **2d**, **2f** and **2i**

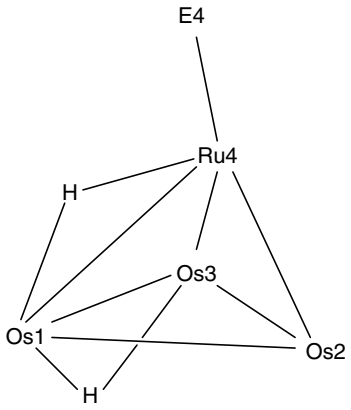

Compound	***Ru*–2a**	**2b**[a]	**2c**	**2d**	**2f**[a]	**2i**
Ligand	PPh_3	$AsPh_3$	$SbPh_3$	P^nBu_3	PCy_2Ph	$P(C_6F_5)_3$
Cone angle (θ) (°)[b]	145	142	138	132	162	184
Electronic parameter (δ_{CO})[c]	4.30	4.16	4.86	5.69	1.24	0.79
Bond parameter						
d(Os1–Os3)	2.9327(4)	2.9314(8)	2.9302(9)	2.9195(6)	2.9239(4)	2.9232(4)
d(Os1–Ru4)	2.9905(3)	2.9864(11)	2.9507(12)	2.9482(8)	2.9688(5)	2.9889(5)
d(Os1–Os2)	2.8150(4)	2.8196(9)	2.8101(8)	2.8050(5)	2.7881(4)	2.8238(4)
d(Os2–Os3)	2.8384(4)	2.8295(9)	2.8253(7)	2.8172(5)	2.8103(4)	2.8206(4)
d(Os2–Ru4)	2.7974(5)	2.7968(12)	2.7846(11)	2.7969(8)	2.8214(5)	2.8115(6)
d(Os3–Ru4)	2.8053(5)	2.8023(11)	2.7926(12)	2.8105(9)	2.8297(5)	2.8257(6)
d(Ru4–E4)	2.3904(15)	2.4764(18)	2.6193(14)	2.374(3)	2.4081(16)	2.3886(18)
∠E4–Ru4–Os1	114.24(4)	113.88(5)	109.62(4)	113.08(8)	114.00(4)	114.90(4)
∠E4–Ru4–Os2	146.03(4)	145.90(5)	142.89(5)	140.05(8)	146.60(4)	128.97(4)
∠E4–Ru4–Os3	149.04(4)	149.18(5)	149.24(5)	155.14(7)	149.28(4)	167.45(5)

[a] Exhibits disorder of metal framework.
[b] Ref. [17].
[c] Ref. [15].

Thus, the preference is electronic. The similarity of the Ru and Os atomic radii predisposes the $RuOs_3$ clusters to positional disorder. In the case of the monosubstituted derivatives, however, the preferential substitution of the ER_3 ligand at the unique Ru vertex generally reduces disorder between Ru and Os vertices; disorder for the Ru-substituted derivatives was modelled only for **2b** and **2f**. This disorder implies that part of the crystal contains molecules substituted at the Os vertex. Evidence for the existence of many of these minor isomers in solution comes from the ^1H and ^{31}P NMR spectra, and is discussed presently.

3.2. Solution structures

In general, the solution spectra suggested that for most of the derivatives, there were more than one isomer in solution. In our tentative assignments of the solution structures, we have assumed that the various isomers could be attributed to different relative arrangements of the phosphorus and hydride ligands only, and that the CO ligands were in rapid exchange. The latter was corroborated by the $^{13}C\{^1H\}$ NMR spectra of **2a** taken at 300 and 223 K, which showed no distinct CO resonances. The IR spectra showed broad, and most often no, bridging carbonyl signals although these groups were present in the solid-state structures, suggesting that CO exchange was fast even on the IR timescale (10^{-11} s compared to $\sim 10^{-5}$ s for NMR). The IR spectrum of **2a** was also recorded in a number of solvents: hexane, toluene, tetrachloromethane, dichloromethane, tetrahydrofuran and acetonitrile. Except for the expected variation in broadness of the peaks, there were no variations with solvent that may suggest a change in isomer distribution with solvent polarity. This was also corroborated by the ^1H NMR spectrum of **2a** in d_8-toluene or CD_3CN, which did not show significant variations in relative peak intensities from those taken in $CDCl_3$, and was in sharp contrast to observations on the $FeRu_3$ system [3a].

The NMR spectra of **2a** have been assigned to the presence of two isomers with structures corresponding to those observed in the solid-state, viz., ***Ru*–2a** and ***Os*–2a**; the assignments are as depicted in Fig. 4, isomers I and II, respectively. The measured T_1's for the hydrides, which

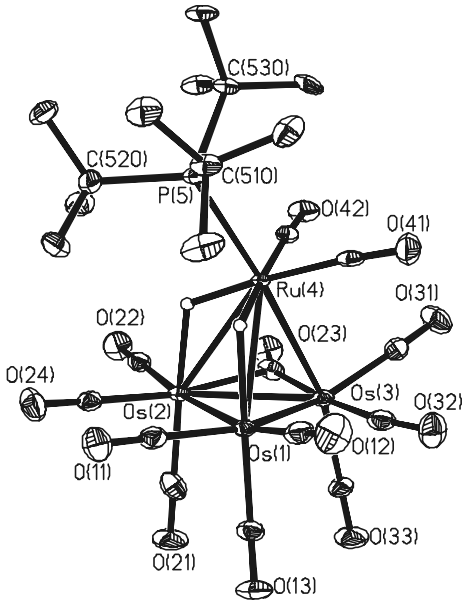

Fig. 3. ORTEP diagram of **2e** (50% thermal ellipsoids) with organic hydrogens omitted. Os(1)–Os(2) = 2.8406(3) Å; Os(1)–Os(3) = 2.8062(3) Å; Os(1)–Ru(4) = 2.9731(5) Å; Os(2)–Os(3) = 2.8079(3) Å; Os(2)–Ru(4) = 3.0045(5) Å; Os(3)–Ru(4) = 2.8168(5) Å; Ru(4)–P(5) = 2.5065(16) Å; ∠Os(1)–Ru(4)–P(5) = 117.54(4)°; ∠Os(2)–Ru(4)–P(5) = 118.34(4)°; ∠Os(3)–Ru(4)–P(5) = 174.81(4)°.

were all ~1.9 s, are also consistent with these structures. We have also earlier on reported on the assignments for the two major isomers of **2b** and **2c** as well as the chemical exchanges that occurred [6]; a third isomer (III) has also been tentatively identified.

The NMR spectra of the trialkylphosphine derivatives **2d**, **2e** and **2h** showed only one isomer each in solution; these were consistent with the solid-state structures persisting in solution (Fig. 4). The different structure adopted by **2e** is presumably the result of the extreme combination of steric and electronic parameters for the P(*t*-Bu)$_3$ ligand: a very large cone angle (182°) and the lowest δ_{CO} value (6.37) [15]. The solution NMR spectra for **2g** showed the presence of a minor isomer (~8% of the major isomer, the ^{31}P and hydride resonances have been correlated by HMBC), which has been tentatively assigned to an isomer III. An EXSY spectrum of **2g** (300 K) also showed that there were exchanges between the hydrides within isomer I, and an isomerisation process between I and III; these exchanges can readily be envisaged to occur via hydride migration from one metal–metal edge to another. Similarly, the solution NMR spectrum for **2i** showed the presence of a minor isomer, in addition to the major isomer I. This minor isomer (~89% of the major isomer) has been tentatively assigned to an isomer of type II; its ^{31}P resonance is ~33 ppm upfield with respect to that for the major isomer, which is indicative that the phosphine ligand is probably bonded to an Os atom. The relative proportion of the two isomers in **2i** is the highest observed for a secondary isomer. Cluster **2i** is also the least soluble and least stable of the monosubstituted derivatives. On standing the NMR sample for a few days, decomposition to the parent cluster **1** and the free ligand was observed.

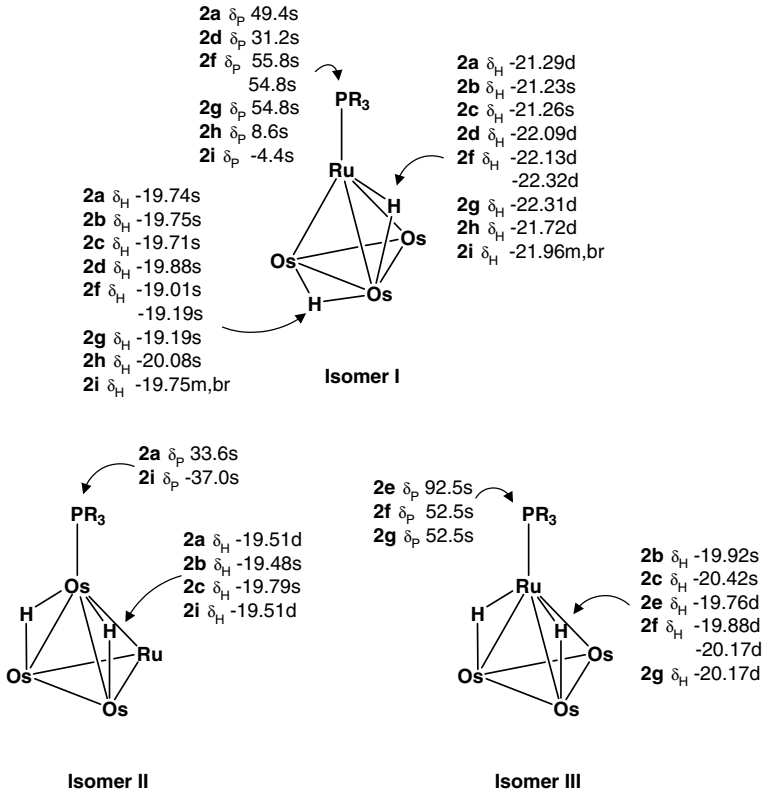

Fig. 4. Solution structures and tentative NMR assignments for the isomers of monosubstituted derivatives **2**.

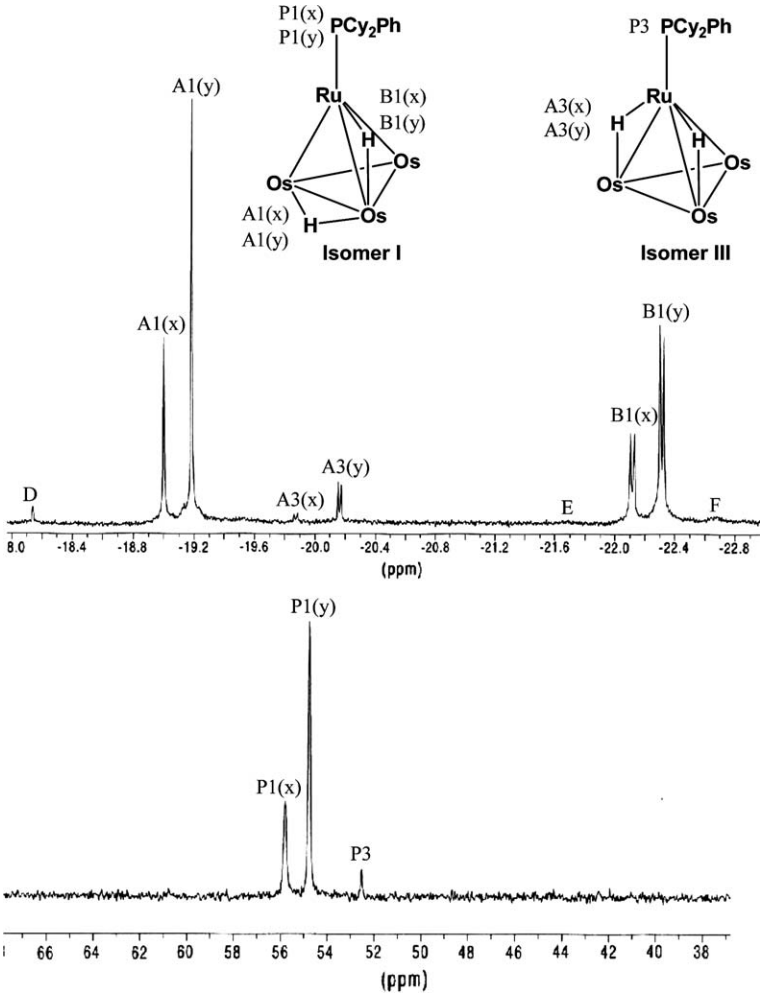

Fig. 5. ^{1}H (top) and $^{31}P\{^{1}H\}$ (bottom) NMR spectra ($CDCl_3$, 300 K) of **2f**. (Inset) Tentative NMR assignments for the isomers of **2f**.

The solution ^{1}H and $^{31}P\{^{1}H\}$ NMR spectra of **2f** turned out to be even more complicated than any of the other monosubstituted derivatives (Fig. 5). The main hydride resonances appeared to occur in pairs (labelled as 'x' and 'y'), while there were three $^{31}P\{^{1}H\}$ resonances. The resonances have been correlated by both ^{1}H COSY and ^{31}P–^{1}H HMBC, and by comparison with the other derivatives have been tentatively assigned as shown. Thus, the major isomer(s) is of type I and the second isomer is of type III. In addition to these, there were also minor resonances (labelled C to E) with low intensities which have not been assigned.

The ^{1}H EXSY spectrum of **2f** showed both isomerisation and hydride exchange processes as those in **2a** (Fig. 6). In addition, exchange between sets (x) and (y) for each of the isomers (crosspeaks marked 'a', 'e', 'g' and 'p' for type I, and 'l' for isomer type III) and between isomers (crosspeaks marked 'c', 'i', 'j' and 'n') were also seen. The former group of exchange crosspeaks allowed us to rule out contamination of **2f** by **2g**; the $^{31}P\{^{1}H\}$ and ^{1}H resonances for the 'y' set of the type I isomer of **2f** were identical to those in **2g**. On lowering the temperature to 273 K and below, the ^{1}H resonances broadened progressively; the slow exchange limit was not observed even at the lowest temperature attainable (223 K). This phenomenon was similarly observed for the disubstituted analogue **3f**, and suggested that it was likely related to the PCy_2Ph ligand.

Since rotation about the P–C bonds was expected to be extremely rapid and not unique to the PCy_2Ph ligand, it could be safely ruled out. Interconversion between the two conformations of cyclohexane, C_6H_{12}, has an enthalpy of activation ($\Delta H^{\ddagger}$) of 10.8 kcal mol^{-1} which should have resulted in coalescence above about 203 K [16]. Furthermore, the difference in conformations was expected to cause a small difference in the $^{2}J_{H-P}$ but not in the chemical shifts. This thus ruled out interconversion between conformations of the Cy rings. The most likely explanation is therefore that of restricted rotation about the P–M bond.

Scheme 1 shows the view down the P–M axis for the two isomers, derived from the X-ray crystal structure of **2f**, with the three positions that the phenyl ring of the ligand may occupy marked as X, Y and Z. A restricted rotation which is sufficiently rapid at ambient temperatures to coalesce the resonances for two of the conformers would be consistent with the integration ratios observed, and also with broadening of the resonances on lowering the temperature – a sign of decoalescence. The same occurs for the type III iso-

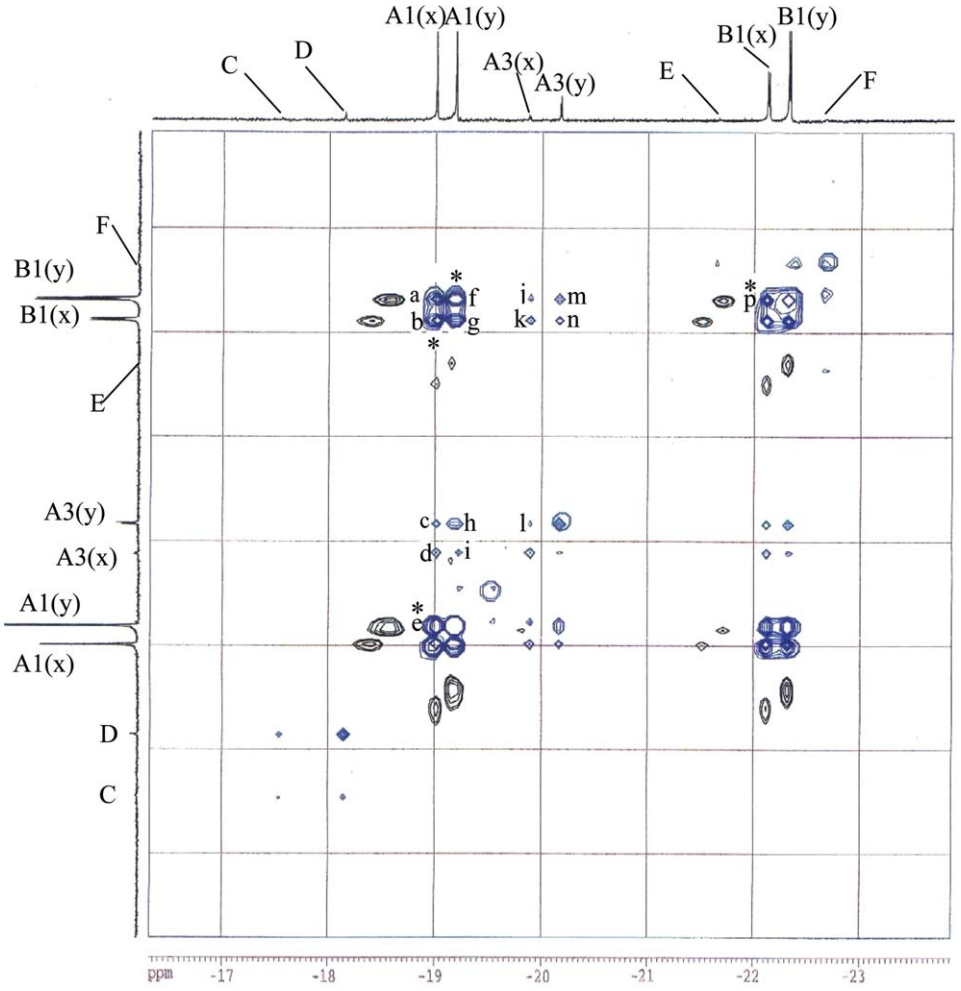

Fig. 6. ^{1}H EXSY spectrum of **2f** in $CDCl_3$ at 300 K ($\tau_m = 0.5$ s). Crosspeaks marked (*) denotes those still present in the EXSY at $\tau_m = 0.05$ and 0.01 s. Exchange crosspeaks labelled: (a) A1(x) ↔ B1(y); (b) A1(x) ↔ B1(x); (c) A1(x) ↔ A3(y); (d) A1(x) ↔ A3(x); (e) A1(x) ↔ A1(y); (f) A1(y) ↔ B1(y); (g) A1(y) ↔ B1(x); (h) A1(y) ↔ A3(y); (i) A1(y) ↔ A3(x); (j) A3(x) ↔ B1(y); (k) A3(x) ↔ B1(x); (l) A3(x) ↔ A3(y); (m) A3(y) ↔ B1(y); (n) A3(y) ↔ B1(x); (p) B1(x) ↔ B1(y).

mer, in which the two expected resonances for the conformers corresponding to the phenyl ring at position X or Y are coalesced at ambient temperatures. On reducing the mixing time for the EXSY spectrum to 0.05 or 0.01 s, only the exchange crosspeaks 'b', 'e', 'f' and 'p', i.e., between conformers and within the main (type I) isomer hydride resonances were retained. This suggests that the restricted ligand rotation occurs at a comparable, but slightly faster, rate to hydride migration; only the latter can result in crosspeaks between the two types of isomers.

In solution, therefore, three types of isomers have been observed for the nine monosubstituted derivatives examined. The number and type of isomers obtained for each compound depended on the nature of the ER_3 ligand used. With the notable exception of **2e**, the most abundant isomer observed is of type I. In this isomer, the hydride bridging the Os–Os edge resonates at lower field (δ −19.1 to −20.1 ppm) compared to that bridging the Ru–Os edge (δ −21.2 to −22.3 ppm); this is also true for the two derivatives (**2b** and **2c**) which have isomers of types II and III. The reverse trend for the relative positions of the hydride shifts is observed in the parent cluster 1.

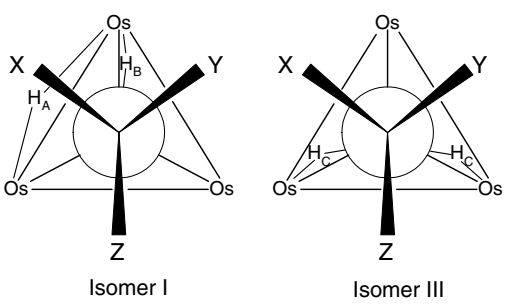

Scheme 1.

4. Concluding remarks

In this study, we have found that the monosubstituted derivatives $RuOs_3(\mu\text{-}H)_2(CO)_{12}(L)$ exhibit isomers which differ in the locations, and relative orientations, of the group 15 ligands and metal hydrides. In contrast to the

related cluster $FeRu_3(\mu\text{-}H)_2(CO)_{13}$, there is no solvent dependence in the isomeric distribution. Substitution appears to be predominantly at the ruthenium vertex. Hydride fluxionality is facile in these clusters, and in the case of the PCy_2Ph ligand, there is also NMR evidence of restricted rotation about the metal–phosphorus bond.

A comparison of the solid-state structures and the solution structures also suggests that there is an interesting correlation between the disorder found in the former and the isomeric distribution in the latter. For instance, in the clusters **2d**–**h** with no known Os-substituted isomers, there is no disorder of the group 15 ligand over Ru and Os. The converse, however, may not be true, i.e., clusters with Os-substituted isomers known in solution may not necessarily give significant disorder of this type, as exemplified by **2c** and **2i**.

Acknowledgement

This work was supported by the National University of Singapore (Research Grant No. R143-000-190-112) and one of us (L.J.P.) thanks the University for a Research Scholarship.

Appendix A. Supplementary information available

CCDC 283356–283361 contains the supplementary crystallographic data for this paper. These data can be obtained free of charge from The Cambridge Crystallographic Data Centre via www.ccdc.cam.ac.uk/data_request/cif. Supplementary data associated with this article can be found, in the online version, at doi:10.1016/j.jorganchem.2006.01.028.

References

[1] G.L. Geoffroy, W.L. Gladfelter, J. Am. Chem. Soc. 99 (1977) 7565.
[2] Some examples: (a) B. Bonelli, S. Brait, S. Deabate, E. Garrone, R. Giordano, E. Sappa, F. Verre, J. Clust. Sci. 11 (2000) 307;
(b) M. Castiglioni, R. Giordano, E. Sappa, J. Organomet. Chem. 491 (1995) 111;
(c) S. Yamamoto, K. Asakura, A. Nitta, H. Kuroda, J. Phys. Chem. 96 (1992) 9565;
(d) S. Yamamoto, Y. Miyamoto, R.M. Lewis, M. Koizumi, Y. Morioka, K. Asakura, H. Kuroda, J. Phys. Chem. 96 (1992) 6367;
(e) S. Aime, M. Cisero, R. Gobetto, D. Osella, A.J. Arce, Inorg. Chem. 30 (1991) 1614;
(f) L. Huang, A. Choplin, J.M. Basset, U. Siriwardane, S.G. Shore, R. Mathieu, J. Mol. Catal. 56 (1989) 1;
(g) S. Dobos, I. Boszormenyi, J. Mink, L. Guczi, Inorg. Chim. Acta 134 (1987) 203;
(h) S. Dobos, A. Beck, S. Nunziante-Cesaro, M. Barbeschi, Inorg. Chim. Acta 130 (1987) 65.
[3] (a) J.R. Fox, W.L. Gladfelter, T.G. Wood, J.A. Smegal, T.K. Foreman, G.L. Geoffroy, I. Tavaniepour, V.W. Day, C.S. Day, Inorg. Chem. 20 (1981) 3214;
(b) W.L. Gladfelter, J.R. Fox, J.A. Smegal, T.G. Wood, G.L. Geoffroy, Inorg. Chem. 20 (1981) 3223;
(c) W.L. Gladfelter, G.L. Geoffroy, Inorg. Chem. 19 (1980) 2574;
(d) J.R. Fox, W.L. Gladfelter, G.L. Geoffroy, Inorg. Chem. 19 (1980) 2579.
[4] H.C. Foley, G.L. Geoffroy, J. Am. Chem. Soc. 103 (1981) 7176.
[5] L. Pereira, W.K. Leong, S.Y. Wong, J. Organomet. Chem. 609 (2000) 104.
[6] L. Pereira, W.K. Leong, J. Organomet. Chem. (accepted).
[7] SMART Version 5.628; Bruker AXS, Inc., Madison, WI, USA, 2001.
[8] SAINT+ Version 6.22a; Bruker AXS, Inc., Madison, WI, USA, 2001.
[9] G.M. Sheldrick, SADABS, 1996.
[10] SHELXTL Version 5.1; Bruker AXS, Inc., Madison, WI, USA, 1997.
[11] A.G. Orpen, XHYDEX; School of Chemistry, University of Bristol, UK, 1997.
[12] S. Aime, W. Dastrù, R. Gobetto, A. Viale, Inorg. Chem. 39 (2000) 2422.
[13] R.H. Crabtree, M. Lavin, Inorg. Chem. 25 (1986) 805.
[14] (a) M.I. Bruce, M.J. Liddell, C.A. Hughes, B.W. Skelton, A.H. White, J. Organomet. Chem. 347 (1988) 157;
(b) M.I. Bruce, M.J. Liddell, C.A. Hughes, J.M. Patrick, B.W. Skelton, A.H. White, J. Organomet. Chem. 347 (1988) 181;
(c) M.I. Bruce, M.J. Liddell, O. Shawkataly, I. Bytheway, B.W. Skelton, A.H. White, J. Organomet. Chem. 369 (1989) 217;
(d) K. Biradha, V.M. Hansen, W.K. Leong, R.K. Pomeroy, M.J. Zaworotko, J. Cluster Sci. 11 (2000) 285.
[15] G.M. Bodner, M.P. May, L.E. McKinney, Inorg. Chem. 19 (1980) 1951.
[16] A. Streitwieser, C.H. Heathcock, Introduction to Organic Chemistry, Macmillan, New York, 1976, p. 614.
[17] C.A. Tolman, Chem. Rev. 77 (1977) 313.